Anomaly in the fine-structure splitting of EPR spectra of Cr^{3+} centres in Tl_2ZnF_4 crystals

2002 J. Phys.: Condens. Matter 14 8613

(http://iopscience.iop.org/0953-8984/14/36/317)

INSTITUTE OF PHYSICS PUBLISHING JOURNAL OF PHYSICS: CONDENSED MATTER

J. Phys.: Condens. Matter **14** (2002) 8613–8623 PII: S0953-8984(02)39831-X

Anomaly in the fine-structure splitting of EPR spectra of Cr^{3+} centres in Tl_2ZnF_4 crystals

M Arakawa[1], **H Ebisu**[2] **and H Takeuchi**[3]

[1] Department of Materials Science and Engineering, Nagoya Institute of Technology, Nagoya 466-8555, Japan
[2] Department of Electrical and Computer Engineering, Nagoya Institute of Technology, Nagoya 466-8555, Japan
[3] Department of Advanced Science and Technology, Toyota Technological Institute, Nagoya 468-8511, Japan

Received 22 July 2002
Published 29 August 2002
Online at stacks.iop.org/JPhysCM/14/8613

Abstract

EPR measurements have been made at room temperature on as-grown single crystals of Tl_2ZnF_4. For crystals doped with Cr^{3+}, signals from the Cr^{3+} centres with monoclinic (centre II) and orthorhombic (centre III) symmetries are observed together with ones from the uncompensated tetragonal centre (centre I). On the basis of spin-Hamiltonian separation analysis, the centre II is ascribed to a Cr^{3+} ion substituted for a Zn^{2+} site with a vacancy at its nearest Tl^+ site. The centre III is ascribed to a Cr^{3+} ion associated with a vacancy at the nearest Zn^{2+} site. Anomalies were revealed in the separated parameters $b_{2a(1)}$ for the centres II, III and in $b_{2a(2)}$ for the centre III, which have about double the magnitude of those in the other layered perovskite fluorides Rb_2ZnF_4, K_2ZnF_4 with different monovalent cations. These anomalies may be due to some effect of the nearest and the next-nearest Tl^+ ions.

1. Introduction

K_2NiF_4-like layered perovskite crystals with space group $I4/mmm$ are interesting because of their close relationship to $KNiF_3$-like cubic perovskite crystals. The layered crystals may be regarded as a two-dimensional network of NiF_6 octahedra sharing corners, in contrast with the three-dimensional network in the cubic perovskite structure. It is known that a Cr^{3+} ion in cubic perovskite crystals ABF_3 substitutes for a host divalent B^{2+} ion. Tetragonal and trigonal Cr^{3+} centres of several kinds are found to be formed in these crystals [1–3], where the excess monovalent positive charge on the Cr^{3+} ion is locally just compensated by a Li^+ (the Cr^{3+}–Li^+ centre) at the nearest B^{2+} site [1] or by a vacancy (the Cr^{3+}–V_A centre) at the nearest A^+ site [2]. In these crystals, tetragonal Cr^{3+} centres with vacancies at the nearest B^{2+} site (the Cr^{3+}–V_B centre) [3] are also formed, though excess positive charge on the Cr^{3+} ion is locally overcompensated by the B^{2+} vacancy.

0953-8984/02/368613+11$30.00

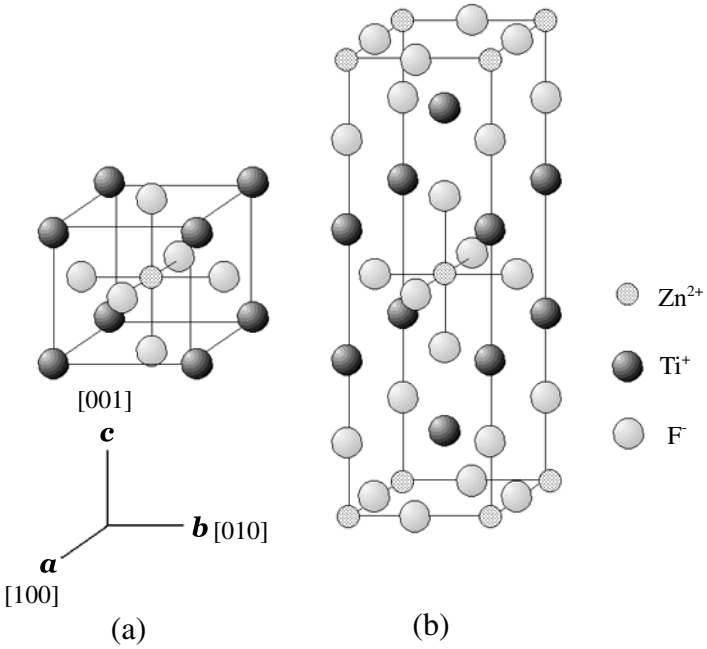

Figure 1. Unit cells of (a) virtual cubic perovskite $TlZnF_3$ crystal and (b) layered perovskite Tl_2ZnF_4 crystal.

In the layered perovskite crystals A_2BF_4, Cr^{3+} ions substitute for B^{2+} ions, similarly to the case for ABF_3 crystals. In A_2BF_4 crystals, EPR spectra of the Cr^{3+}–V_B and the Cr^{3+}–Li^+ centres with orthorhombic symmetry have been observed together with a spectrum of the Cr^{3+} ion with tetragonal symmetry without any local compensation in its immediate neighbourhood (the uncompensated centre) [4–7]. For these centres the relationships between the parameters b_2^m ($m = 0, 2$) and the local environments around Cr^{3+} ions were deduced by separating the fine-structure terms into two uniaxial terms along the c-axis and along the Cr^{3+}–V_B (or the Cr^{3+}–Li^+) pair direction using the spin-Hamiltonian separation method [4–8]. The structure of the centre in A_2BF_4 crystal can be considered by comparing each separated parameter with the axial parameter for the uncompensated centre observed in the same host crystal and with that for the same kind of Cr^{3+}–V_B (or Cr^{3+}–Li^+) centre in ABF_3 crystal.

It is well known that the structures of the compounds ABF_3 are closely related to the tolerance factor t $(=(r_A + r_F)/\sqrt{2}(r_B + r_F))$. Babel [9] reported that the cubic perovskite structure occurs in the range of the tolerance factor $0.88 \leqslant t \leqslant 1.00$ and the hexagonal $BaTiO_3$-type structure occurs in the range of $1.00 \leqslant t \leqslant 1.06$. On the other hand, A_2BF_4 crystals have the layered perovskite structure over the range of the tolerance factor corresponding to the cubic perovskite and hexagonal structure of ABF_3 crystals. Crystals of Tl_2MgF_4 and Tl_2ZnF_4 have the layered perovskite structure, in contrast with the hexagonal structure for $TlMgF_3$ ($t = 1.03$) and $TlZnF_3$ ($t = 1.01$) crystals [9]. Figure 1 shows the unit cell of layered perovskite Tl_2ZnF_4 crystal, together with the cubic perovskite structure considered virtually. It must be emphasized that we can obtain the information on the charge-compensated centres formed in the virtual cubic perovskite crystal in figure 1(a) using the spin-Hamiltonian separation method, although the cubic perovskite structure does not occur in real $TlZnF_3$ crystal.

Recently, we reported EPR results for tetragonal and orthorhombic centres observed in Tl_2MgF_4 and Tl_2ZnF_4 crystals co-doped with Cr^{3+} and Li^+ [10]. It was found that the spectra of

tetragonal centres exhibit anomalously large fine-structure splittings, which were about double those in K_2MF_4 and Rb_2MF_4 (M = Mg, Zn). Using the spin-Hamiltonian separation analysis, the separated parameter corresponding to the uncompensated centre was in good agreement with the fine-structure parameter for the tetragonal centre. The tetragonal centre was identified unambiguously as the uncompensated centre in spite of the anomalously large fine-structure splittings. The orthorhombic centre was ascribed to a Cr^{3+} ion associated with a Li^+ ion at the nearest Zn^{2+} site (centre IV) [10].

In this paper, we will report EPR results for monoclinic (centre II) and orthorhombic (centre III) centres newly observed in Tl_2ZnF_4 single crystals doped only with Cr^{3+}. For identification of the centres II and III, the second-rank fine-structure terms will be analysed using the spin-Hamiltonian separation method. We will discuss the separated parameters by comparing with recent results for the centres I and IV in Tl_2ZnF_4 and with those obtained from other perovskite crystals.

2. Experimental procedures and results

Single crystals of Tl_2ZnF_4 were grown in graphite crucibles by the Bridgman technique. Powder of CrF_3 was added to starting mixtures of ZnF_2 and TlF. The crystals obtained are cleaved easily in the c-plane. The measurements were made at room temperature using a JES-FE1XG ESR spectrometer operating in the X band at the Centre for Instrumental Analysis at Nagoya Institute of Technology.

For an as-grown crystal of Tl_2ZnF_4 doped with Cr^{3+}, signals from two kinds of new centre were observed at room temperature, together with those from the centre I previously reported [10]. A recorder trace of the EPR signals with $\boldsymbol{H} \parallel \boldsymbol{a}$ at room temperature is shown in figure 2(a). Figure 2(b) shows the recorder trace of the EPR signals obtained for another crystal co-doped with Cr^{3+} and Li^+ used for EPR observation in the previous work [10]. Signals from the centres I, II, III and IV are marked with Roman numerals in figure 2. The centres II and III disappear for the crystals co-doped with Cr^{3+} and Li^+, as seen from figure 2(b). The centre IV is observed selectively in the Li^+ co-doped crystals.

In figure 3 signals observed at room temperature are plotted as open triangles for the centre I, open circles for the centre II and open squares for the centre III against the external field direction in the c-plane. The spectrum of the centre I show no variation in this plane. This indicates that the centre I has tetragonal symmetry about the crystalline c-axis.

The signals from the centre II have a set of branches, as seen in figure 3. The branches have peaks and troughs in the [110] field direction and coincide with each other in the [100] direction. From the field direction dependence in the $(\bar{1}10)$ plane, we see that the signals from the centre II show extremes for a direction declined by about 36° from the c-axis in the plane. This makes it clear that the spectra of the centre II have monoclinic symmetry. Each branch corresponds to the association of some charge compensator in one of the $\langle 110 \rangle$ symmetry planes.

In contrast with those for the centre II, the branches for the centre III have peaks and troughs in the [100] direction and coincide with each other in the [110] direction as seen from figure 3. Another coincidence of the branches is observed in the [001] field direction. This makes it clear that the spectra of the centre III have orthorhombic symmetry due to some charge compensator along a crystalline axis in the c-plane. The disappearance of the centre III in Li^+ co-doped crystals and the similarity of the field direction dependence to that of the centre IV indicate that the charge compensation for the centres III takes place at the same site as that of Li^+ for the centre IV.

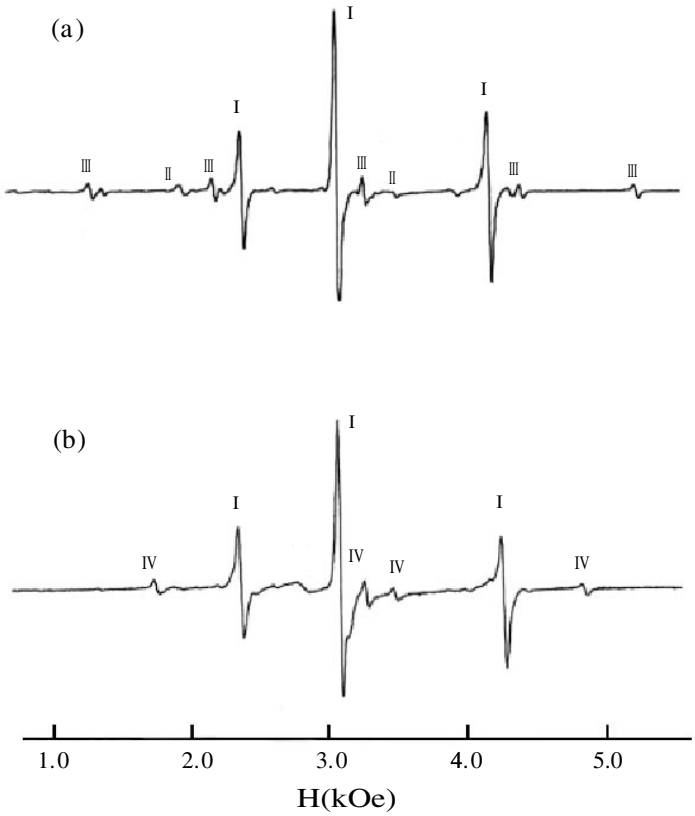

Figure 2. Observed EPR spectra of the Cr^{3+} centres at room temperature with $\boldsymbol{H} \parallel [100]$ in Tl_2ZnF_4 (a) doped only with Cr^{3+} and (b) co-doped with Cr^{3+} and Li^+. The labels II and III denote respectively the signals from new monoclinic and orthorhombic centres. Signals from the centres I and IV previously reported [10] are denoted by I and IV.

The spectra of the centres II and III can be described by the following spin Hamiltonian:

$$\mathcal{H} = g_z\beta S_z B_z + g_x\beta S_x B_x + g_y\beta S_y B_y + \tfrac{1}{3}[b_2^0 O_2^0 + b_2^2 O_2^2], \tag{1}$$

where O_2^0 and O_2^2 are the Stevens operators defined by Abragam and Bleaney [11]. For the centre II, the spin Hamiltonian is described in the coordinate system where the z-axis is declined at an angle θ from the c-axis in the $(\bar{1}10)$ symmetry plane and the x-axis is in the same plane. For the centres III, the z-axis is chosen to be parallel to the a-axis where the spectrum shows maximum fine-structure splitting, and the x-axis is parallel to the b-axis.

Each spectrum observed was fitted to the spin Hamiltonian by the direct matrix diagonalization method. By this method, relative signs among b_2^m-parameters can be determined uniquely. The sign of b_2^0 for the centre II is selected to be negative as the value of $g_z - (g_x + g_y)/2$ is negative. On the other hand, the signs of b_2^0 for the centres III and IV are selected to be positive as the values of $g_z - (g_x + g_y)/2$ are positive, similarly to the cases for other layered perovskite fluorides [8]. The spin-Hamiltonian parameters obtained are listed in table 1 together with those obtained previously for the centres I and IV [10]. The sign of θ for the centre II cannot be determined by the matrix diagonalization method. It was determined by the spin-Hamiltonian separation analysis, to be mentioned in the following section. Dotted curves in figure 3 show the theoretical curves calculated using the spin-Hamiltonian parameters listed

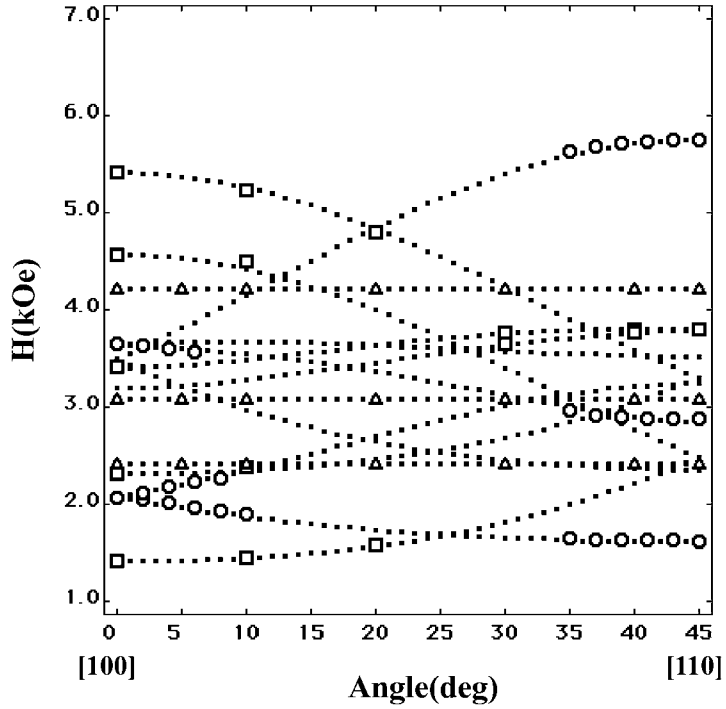

Figure 3. Angular variation of the signals I, II and III labelled in figure 2(a) with $\boldsymbol{H}$ in the c-plane. Open circles are due to the centre II, open squares are due to the centre III and open triangles are due to the centre I. Dotted curves denote the resonance fields calculated using the parameters listed in table 1.

Table 1. Spin-Hamiltonian parameters for several kinds of Cr^{3+} centre observed in Tl_2ZnF_4. The positive sign of θ for the centre II is reasonable, as mentioned in section 4. The units are 10^{-4} cm^{-1} for b_0^2 and b_2^2.

Centre	g_x	g_y	g_z	b_2^0	b_2^2	θ (deg)
I[10)]	1.9724(6)	1.9724(6)	1.9715(6)	−866.1(5)	—	—
II	1.9810(5)	1.9772(2)	1.9629(6)	−1507.9(8)	−706.1(6)	±36.3(1)
III	1.972(1)	1.972(1)	1.975(1)	924.5(8)	−156(1)	—
IV[10)]	1.971(1)	1.970(1)	1.9734(8)	684.6(7)	529(1)	—

in table 1. Good agreement of the calculated values of the resonant fields with experimental ones is obtained.

3. Spin-Hamiltonian separation analysis

The spin-Hamiltonian separation method has been successfully applied to identify the magnetic impurity centres in low-symmetry crystals [4–8]. For identification of charge-compensated centres in layered perovskite fluorides, the surroundings of the centres with lower symmetry can be interpreted by separating them into two configurations of surrounding ions. One is a similar configuration to that of the uncompensated centre in the same host crystal. The other is a configuration corresponding to the same kind of charge-compensated centre in the

Table 2. Values of $b_{2a(1)}$ derived for the orthorhombic centres III, IV and values of b_2^0 for the centres I in several layered perovskite fluorides. The units are 10^{-4} cm^{-1} for the fine-structure parameters.

Crystal	a (Å)	c (Å)	b_2^0(I)	$b_{2a(1)}$(II)	$b_{2a(1)}$(III)	$b_{2a(1)}$(IV)
K_2MgF_4	3.9704	13.176[13)]	−419[4)]	−590.7	−443[7)]	−413.7[7)]
Tl_2MgF_4	4.007	14.43[9)]	−1041.7[10)]	—	—	−1042.9[10)]
Rb_2MgF_4	4.0584	13.7991[13)]	−526.1[7)]	—	−577.6[7)]	−564.0[7)]
K_2ZnF_4	4.0548	13.096[13)]	−381[4)]	−586.5	−402[5)]	−386[5)]
Tl_2ZnF_4	4.105	14.10[9)]	−866.1[10)]	−838.9	−872.5	−860.9[10)]
Rb_2ZnF_4	4.136	13.706[13)]	−369.0[6)]	—	−394.7[6)]	−410.8[6)]
K_2CdF_4	4.3612	13.266[13)]	−643.1[14)]	—	−623.3[14)]	—
Rb_2CdF_4	4.4017	13.938[13)]	−666.4[6)]	—	−665.4[6)]	−637.7[6)]
Cs_2CdF_4	—	—	−702.0[6)]	—	−740.9[6)]	−733.4[6)]

cubic perovskite crystals composed of the same cations. The spectra of the centres II and III having lower symmetry than the tetragonal one in the same host crystal show that these centres are perturbed by some charge compensator nearby. The fine-structure parameters for the charge-compensated centres can be considered by separating the second-rank fine-structure terms into two uniaxial terms with the parameters $b_{2a(1)}$ along the c-axis and $b_{2a(2)}$ along the direction to the charge compensator. The separated axial parameters $b_{2a(1)}$ are comparable with the parameter b_2^0 for the uncompensated centre in the same host crystal. The other axial parameter, $b_{2a(2)}$, is compared with the parameter for the centre associated with the same kind of charge compensator in the cubic perovskite crystal.

For the monoclinic centre II the main principal axis (the z-axis) of the fine-structure terms is found to be declined by 36.3° from the c-axis in the $(\bar{1}10)$ plane, as shown in table 1. The excess positive charge on the Cr^{3+} ion is assumed to be compensated locally by a vacancy at the nearest Tl^+ site along the [111] direction in this symmetry plane. So, we try to separate the fine-structure terms into two uniaxial terms as follows:

$$b_2^0 O_2^0(z) + b_2^2 O_2^2(x, y) = b_{2a(1)} O_2^0(z') + b_{2a(2)} O_2^0(z''), \tag{2}$$

where the z'-axis is parallel to the c-axis and the z''-axis is assumed to be declined by 54.7° from the c-axis in the $(\bar{1}10)$ plane. Using the transformation properties of the Stevens operators given by Rudowicz [12], we can deduce the following conditions that satisfy equation (2):

$$b_{2a(1)} = \tfrac{1}{2}(3\cos^2\theta - 1)b_2^0 + \tfrac{1}{2}\sin^2\theta b_2^2, \tag{3}$$

$$b_{2a(2)} = \tfrac{3}{2}\sin^2\theta b_2^0 + \tfrac{1}{2}(\cos^2\theta + 1)b_2^2 \tag{4}$$

and

$$\sin 2\theta = \frac{2\sqrt{2}b_{2a(2)}}{3b_2^0 - b_2^2}. \tag{5}$$

We can calculate the separated axial parameters $b_{2a(1)}$ and $b_{2a(2)}$ from equations (3) and (4) using the experimental values of b_2^0, b_2^2 and θ listed in table 1. The values obtained are tabulated in tables 2 and 3. The sign of the angle θ is determined as positive from equation (5). The negative value of $b_{2a(2)}$ is consistent with the positive sign of θ, since $3b_2^0 - b_2^2 < 0$ as seen from table 1.

We also analyse the orthorhombic centres III using the spin-Hamiltonian separation method. We separate the second-rank fine-structure terms into a uniaxial term with the parameters $b_{2a(1)}$ along the crystalline c-axis (the y-axis) and a uniaxial term with $b_{2a(2)}$

Table 3. Values of $b_{2a(2)}$ derived for the monoclinic centres II in several layered perovskite fluorides. The fourth column gives the values of b_2^0 for the trigonal Cr^{3+}–V_K centres in the corresponding cubic perovskite fluorides. The units are 10^{-4} cm^{-1}.

Crystal	$b_{2a(2)}$	Crystal	b_2^0	Reference
K_2MgF_4	−1411.3	$KMgF_3$	−1528	[2]
K_2ZnF_4	−1573.5	$KZnF_3$	−1613	[2]
Tl_2ZnF_4	−1375.1	$TlZnF_3$	—	This work

Table 4. Values of $b_{2a(2)}$ derived for the orthorhombic centres III and IV in the layered perovskite fluorides A_2MF_4. The Δb_{2a} column gives the values of the difference $b_{2a(2)}(\mathrm{III}) - b_{2a(2)}(\mathrm{IV})$. The units are 10^{-4} cm^{-1}.

A_2MF_4	$b_{2a(2)}$(III)	$b_{2a(2)}$(IV)	Δb_{2a}
K_2MgF_4	−565[7]	−470.3[7]	−94.7
Tl_2MgF_4	—	−644.3[10]	—
Rb_2MgF_4	−583.8[7]	−610.2[7]	+26.4
K_2ZnF_4	−424[5]	−374[5]	−50
Tl_2ZnF_4	−976.5	−508.3[10]	−468.2
Rb_2ZnF_4	−408.3[6]	−455.4[6]	+47.1
K_2CdF_4	−346.9[14]	—	—
Rb_2CdF_4	−442.6[6]	−584.7[6]	+142.1
Cs_2CdF_4	−503.1[6]	−710.8[6]	+207.7

along the crystalline b-axis (the x-axis) in the c-plane. The fine-structure terms in the x, y, z coordinate system can be written as follows:

$$b_2^0 O_2^0(z) + b_2^2 O_2^2(x, y) = b_{2a(1)} O_2^0(y) + b_{2a(2)} O_2^0(x). \tag{6}$$

The term $b_{2a(1)} O_2^0(y)$ denotes the uniaxial term, about the y-axis, where $O_2^0(y) = 3S_y^2 - S(S+1)$. Equation (6) is valid when the following conditions are satisfied:

$$b_{2a(1)} = -b_2^0 - \tfrac{1}{3}b_2^2, \qquad b_{2a(2)} = -b_2^0 + \tfrac{1}{3}b_2^2. \tag{7}$$

Values of the separated axial parameters $b_{2a(1)}$ and $b_{2a(2)}$ calculated from the experimental values of b_2^0 and b_2^2 listed in table 1 are tabulated in tables 2 and 4.

4. Discussion

4.1. Centre I

The signals from the centre I with tetragonal symmetry were observed with large intensity for both crystals doped with Cr^{3+} and co-doped with Cr^{3+} and Li^+ as shown in figure 2. In table 2 the separated parameters $b_{2a(1)}$ obtained from the centres II, III and IV in Tl_2ZnF_4 are listed together with those for other layered perovskite fluorides reported previously [4, 5, 7, 13]. The fine-structure parameters b_2^0 for the centres I are also listed in this table for comparison. All separated parameters $b_{2a(1)}$ for the centres II, III and IV in Tl_2ZnF_4 have values close to the b_2^0-parameter for the centre I in the same host crystal. The result indicates that the separations for the centres II and III made in section 3 are appropriate. This makes it possible to consider the parameter $b_{2a(2)}$ as the information on b_2^0 for the same kind of charge-compensated centre in the virtual cubic perovskite $TlZnF_3$ crystal, although the real structure of $TlZnF_3$ is hexagonal. It may be safely said that the centre I is ascribable to a Cr^{3+} ion substituted for the Zn^{2+} site

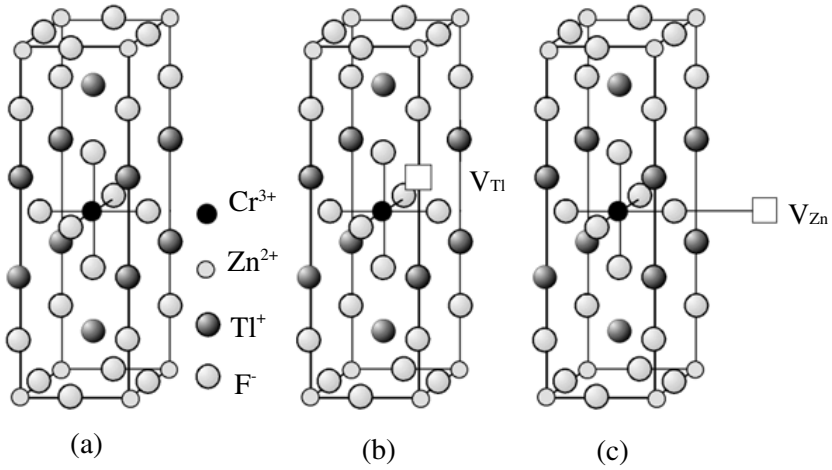

Figure 4. Schematic models for (a) the centre I, (b) the centre II and (c) the centre III.

without any charge compensator in its immediate neighbourhood. A schematic model for the centre I is shown in figure 4(a).

The magnitude of the parameter b_2^0 for the centre I for Tl_2ZnF_4 is about double that for Rb_2ZnF_4. This tendency also holds between Tl_2MgF_4 and Rb_2MgF_4 crystals. The lattice parameters a are almost the same for the two crystals. The difference in b_2^0-parameters comes from the difference in monovalent cations of the host crystals. As seen from table 2, the lattice parameters c for Tl_2ZnF_4 and Tl_2MgF_4 are larger than those for Rb_2ZnF_4 and Rb_2MgF_4 although the ionic radius (1.47 Å) of Tl^+ is the same as that of Rb^+. The effect of Tl^+ ions on the local environment around the Cr^{3+} ion may be related to the difference in lattice parameter c.

4.2. Centre II

The parameters $b_{2a(2)}$ derived from the centre II are listed in table 3 together with those derived from the monoclinic centres reported in the layered perovskite fluorides K_2MF_4 (M = Mg, Zn) [4]. The b_2^0 for the trigonal Cr^{3+}–V_K centres in the cubic perovskite crystals KMF_3 [2] are also listed for comparison. The value of $b_{2a(2)}$ for Tl_2ZnF_4 is close to $b_{2a(2)}$ for K_2MF_4 and to b_2^0 for the Cr^{3+}–V_K centres in KMF_3. This shows that the centre II in Tl_2ZnF_4 can be considered to be associated with the same kind of charge compensator as those in other crystals. So, the centre II can be ascribed to a Cr^{3+} ion at the Zn^{2+} site associated with a vacancy at the nearest Tl^+ site, as shown in figure 4(b).

It must be emphasized that the relationship between the direction of the principal z-axis in the spin Hamiltonian and the configuration of the centre with charge compensator can be clarified by spin-Hamiltonian separation analysis. As mentioned in section 3, the sign of the angle θ in table 1 is determined as positive. This shows that the direction of the z-axis for the centre II is declined from the [001] axis by an angle of about 36° in the $(\bar{1}10)$ plane toward the *same* direction to the vacancy at the nearest Tl^+ site.

4.3. Centre III

The orthorhombic centres observed in several layered perovskite fluorides have been identified using the spin-Hamiltonian separation analysis [4, 5, 7, 12], where the excess positive charge

Table 5. Values of b_2^0 for the Cr^{3+}–V_M and the Cr^{3+}–Li^+ centres in cubic perovskite fluorides AMF_3. The Δb_2^0 column gives the values of the difference $b_2^0(V_M) - b_2^0(Li)$. Asterisks denote $TlMgF_3$, $TlZnF_3$ and $RbMgF_3$ having not cubic perovskite structures but hexagonal ones. The units are 10^{-4} cm^{-1}.

AMF_3	$b_2^0(V_M)$	$b_2^0(Li^+)$	Δb_2^0
$KMgF_3$	—	—	—
$TlMgF_3^*$	—	—	—
$RbMgF_3^*$	—	—	—
$KZnF_3$	-542.1[3)]	-508.0[3)]	-34.1
$TlZnF_3^*$	—	—	—
$RbZnF_3$	-535[6)]	-594.4[6)]	$+59.4$
$KCdF_3$	-511.3[3)]	-621.2[3)]	$+109.9$
$RbCdF_3$	-569.3[3)]	-743.9[3)]	$+174.6$
$CsCdF_3$	-629.3[3)]	-858.8[3)]	$+229.5$

on the Cr^{3+} at a divalent cation site is compensated by a vacancy (centre III) or Li^+ (centre IV) at the nearest divalent cation site. As shown in table 4, the separated parameters $b_{2a(2)}$ for the centres III and IV in A_2MF_4 are compared with the parameters b_2^0 for the Cr^{3+}–V_M and Cr^{3+}–Li^+ centres. As $TlZnF_3$ has not the cubic perovskite structure but the hexagonal one, the separated parameters $b_{2a(2)}$ for the centres III and IV in Tl_2ZnF_4 give additional information on the parameter b_2^0 for the centres formed virtually in the cubic perovskite structure.

The value of $b_{2a(2)}$ for the centre IV in Tl_2ZnF_4 is close to $b_{2a(2)}$ for the centres IV in other crystals, as seen from table 4. So, the centre IV in Tl_2ZnF_4 can be ascribed to a Cr^{3+} ion associated with a Li^+ ion at the nearest Zn^{2+} site for compensation of excess positive charge on a Cr^{3+} at the Zn^{2+} site [4]. As mentioned in section 3, the charge compensation in the centres III and IV takes place at the same site in this crystal. The centre III can be ascribed to a Cr^{3+} ion associated with a vacancy at the nearest Zn^{2+} site in the c-plane, as shown in figure 4(c).

The negative sign of b_2^0 for the centre I in table 2 arises from the deviation of the apical ligand F^- ions on the c-axis toward the Cr^{3+} ion, resulting in a compressed ligand octahedron along the c-axis. The magnitudes of the parameter $b_{2a(2)}$ derived for the centres IV in the layered perovskite fluoride are slightly smaller than those of the parameter b_2^0 for the corresponding centres in the perovskite fluorides, as seen from tables 4 and 5. Smaller $|b_{2a(2)}|$ values suggest that two apical ligand F^- ions on the c-axis prevent the deviation of the intervening F^- ion between the Cr^{3+} and Li^+ ions toward the Cr^{3+} ion by F^-–F^- Coulomb repulsion.

The dependence of the difference $\Delta b_{2a(2)}$ ($=b_{2a(2)}(\mathrm{III}) - b_{2a(2)}(\mathrm{IV})$) on the metal–ligand distance in the c-plane is shown in figure 5. A similar dependence of the difference Δb_2^0 ($=b_2^0(V_M) - b_2^0(Li)$) for cubic perovskite fluorides is also shown in the figure. The dependence of $\Delta b_{2a(2)}$ on M–F distance is similar to that of Δb_2^0 except for Tl_2ZnF_4, as seen from figure 5. For Tl_2ZnF_4 the value of the difference $\Delta b_{2a(2)}$ has negative sign and has an anomalously large magnitude. This result arises from $b_{2a(2)}$ for the centre III in Tl_2ZnF_4 having an anomalously large magnitude in contrast with that for the centre IV, as seen from table 4. The magnitude of $b_{2a(2)}$ for the centre III is about double those of Rb_2ZnF_4 and K_2ZnF_4, similarly to the case for b_2^0 for the centre I.

The anomaly of b_2^0 for the centre I may arise from some effect on the local distortion of the apical ligand F^- ions by the nearest Tl^+ ions along the $\langle 111 \rangle$ axes and the next-nearest Tl^+ ions along the c-axis. The anomalously large magnitude of $b_{2a(2)}$ for the centre III may arise from some effect of the nearest Tl^+ ions on the local distortion of the intervening F^- ion between the Cr^{3+} ion and the vacancy at the nearest Zn^{2+} site. The value of $b_{2a(2)}$ for the centre

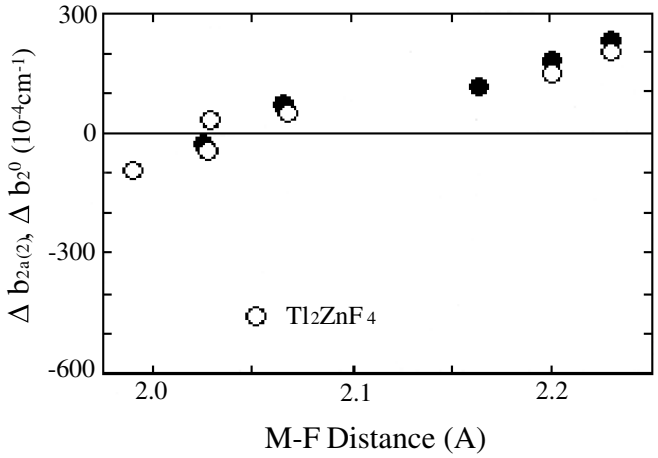

Figure 5. Dependences of $\Delta b_{2a(2)}$ and Δb_2^0 on the metal–ligand distance in the *c*-plane. Open circles show $\Delta b_{2a(2)} = (b_{2a(2)}(\mathrm{III}) - b_{2a(2)}(\mathrm{IV}))$ for layered perovskite fluorides. Closed circles show $\Delta b_2^0 = (b_2^0(\mathrm{V_M}) - b_2^0(\mathrm{Li}))$ for cubic perovskite fluorides.

II with a vacancy at the nearest Tl^+ site shows no anomaly, as seen from table 3. We conclude that the anomaly for the centres I and III may arise from some effect of monovalent Tl^+ ions nearby. The anomaly in $b_{2a(2)}$ for the centre III suggests that a similar effect of Tl^+ ions may take place in b_2^0 for the Cr^{3+}–V_M centres in cubic perovskite $TlMF_3$.

5. Conclusions

Three kinds of EPR spectrum for the Cr^{3+} centres (I, II, III) have been observed for Tl_2ZnF_4 crystals doped with Cr^{3+}. One comprises the signals from the tetragonal Cr^{3+} centre (I) with strong intensity and the others comprise those from the monoclinic (II) and the orthorhombic (III) centres. For the centres II and III the fine-structure parameters are considered using spin-Hamiltonian separation analysis. The separated parameters $b_{2a(1)}$ for centres II and III have values close to the parameter b_2^0 for the centre I. The monoclinic centre II is ascribed to a Cr^{3+} ion associated with the nearest Tl^+ vacancy (the Cr^{3+}–V_{Tl} centre). The orthorhombic centre III is ascribed to a Cr^{3+} ion associated with the nearest Zn^{2+} vacancy in the *c*-plane (the Cr^{3+}–V_{Zn} centre).

Anomalies are found in b_2^0 for the centre I, in the separated parameters $b_{2a(1)}$ for the centres II and III and in $b_{2a(2)}$ for the centre III. The fine-structure parameters have at least double the magnitude of those for Rb_2ZnF_4 and K_2ZnF_4. The value of $b_{2a(2)}$ for the centre II with a vacancy at the nearest Tl^+ site shows no anomaly compared with those for the same kind of the centre in cubic and layered perovskite fluorides. The anomaly of b_2^0 for the centre I may arise from some effects of the nearest and the next-nearest Tl^+ ions on the distortion of apical ligand F^- ions along the *c*-axis. The anomaly of $b_{2a(2)}$ for the centre III may arise from some effect of the nearest Tl^+ ions on the distortion of the intervening F^- ion between the Cr^{3+} and the vacancy at the nearest Zn^{2+} site.

The parameters $b_{2a(2)}$ for Tl_2ZnF_4 can be considered as information on b_2^0 for the same kind of centre formed in virtual cubic $TlZnF_3$ crystal, although the real crystal of $TlZnF_3$ has the hexagonal structure. The anomaly of $b_{2a(2)}$ for the centre III suggests that the effect of the Tl^+ ions is on b_2^0 for the Cr^{3+}–V_M centres in cubic perovskite $TlMF_3$. The Tl^+ ions in the

crystals may cause local distortions around the Cr^{3+} ion different from those in the crystals with other monovalent cations such as Rb^+, K^+ and Cs^+.

Acknowledgments

The authors offer appreciative thanks to Miss T Matusima and Mr T Nakano for their help in the EPR experiments and analysis.

References

[1] Rousseau J J, Gesland J Y, Binois M and Fayet J C 1974 *C. R. Acad. Sci., Paris* B **279** 103
[2] Patel J L, Davies J J, Cavenett B C, Takeuchi H and Horai K 1976 *J. Phys. C: Solid State Phys.* **9** 129
[3] Takeuchi H and Arakawa M 1984 *J. Phys. Soc. Japan* **53** 376
[4] Takeuchi H, Arakawa M, Aoki H, Yosida T and Horai K 1982 *J. Phys. Soc. Japan* **51** 3166
[5] Takeuchi H and Arakawa M 1983 *J. Phys. Soc. Japan* **52** 279
[6] Arakawa M, Ebisu H and Takeuchi H 1986 *J. Phys. Soc. Japan* **55** 2853
[7] Arakawa M, Ebisu H and Takeuchi H 1988 *J. Phys. Soc. Japan* **57** 2801
[8] Takeuchi H and Arakawa M 1994 *J. Phys.: Condens. Matter* **6** 3253
[9] Babel D 1967 *Struct. Bonding* **3** 1
[10] Arakawa M, Ebisu H and Takeuchi H 2002 *Proc. APES'01: 3rd Asia–Pacific EPR/ESR Symp.* (Amsterdam: Elsevier) at press
[11] Abragam A and Bleaney B 1970 *Electron Paramagnetic Resonance of Transition Ions* (Oxford: Clarendon)
[12] Rudowicz C 1985 *J. Phys. C: Solid State Phys.* **18** 1415
[13] Schrama A H M 1973 *Physica* **68** 279
[14] Arakawa M, Ebisu H and Takeuchi H 1988 *J. Phys. Soc. Japan* **57** 3573